

Percolation transition of hydration water at hydrophilic surfaces

A. Oleinikova, I. Brovchenko and A. Geiger

Physical Chemistry, University Dortmund, Otto-Hahn-Str.6, D-44221

Abstract

An analysis of water clustering is used to study the quasi-2D percolation transition of water adsorbed at planar hydrophilic surfaces. Above the critical temperature of the layering transition (quasi-2D liquid-vapor phase transition of adsorbed molecules) a percolation transition occurs at some threshold surface coverage, which increases with increasing temperature. The location of the percolation line is consistent with the existence of a percolation transition at the critical point. The percolation threshold at a planar surface is weakly sensitive to the size of the system when its lateral dimension increases from 80 to 150 Å. The size distribution of the largest water cluster shows a specific two-peaks structure in a wide range of surface coverage : the lower- and higher-size peaks represent contributions from non-spanning and spanning clusters, respectively. The ratio of the average sizes of spanning and non-spanning largest clusters is about 1.8 for all studied planes. The two-peak structure becomes more pronounced with decreasing size of the planar surface and strongly enhances at spherical surfaces.

Key words: percolation transition, hydration water, clustering

PACS: 64.60Ak, 87.15Aa

1 Introduction

The existence of an infinite (spanning) network of hydrogen-bonded water molecules strongly affects the properties of aqueous systems and plays an important role in various technological and biological processes. In bulk liquid water such a three-dimensional network exists up to the liquid-vapor critical point [1,2,3]. In the supercritical region a spanning water network appears via

Email address: alla.oleinikova@heineken.chemie.uni-dortmund.de (A. Oleinikova).

a percolation transition at some threshold value of the density, which increases with increasing temperature [4,5]. In aqueous solutions with rather hydrophilic solute, the formation of an infinite water network with increasing water content also occurs via a percolation transition [6,7]. Whereas in solutions with rather hydrophobic solute, the formation of a spanning water network is preceded by the liquid-liquid phase separation [8]. In an aqueous system with constituents, which are noticeably larger than water molecules, obviously, that spanning hydrogen-bonded network of water molecules should be formed rather via a 2D, than via a 3D percolation transition. Indeed, the percolation transition of water was found to be quasi-2D even in a solution of such a relatively small molecule, as tetrahydrofuran [6]. The two-dimensional character of the water percolation transition in aqueous systems should gain more importance with increasing size of the solutes.

Water at the surface of biomolecules (so-called hydration or biological water) strongly influences their structural and dynamical properties. In particular, the existence of a spanning network of hydration water in biosystems enables their biological functions [9,10]. The transformation from an ensemble of finite water clusters to an infinite water network with increasing hydration level occurs via a percolation transition, which was found to be two-dimensional in experiments and computer simulations of various biosystems (see [11,12] and references therein).

Despite the crucial role of the percolation of hydration water for the onset of biological activity, it was not studied yet even for the simplest model systems. The main goal of our paper is to study the (2D) percolation transition of water at smooth planar hydrophilic surfaces in order to create a basis for subsequent investigations of the percolation of hydration water in more complex, first of all biological, systems. Strictly speaking, such a transition is quasi-2D, since even at a smooth surface the adsorbed water molecules are not restricted to a single plane parallel to the adsorbate surface. Therefore, some deviations of the percolation transition of hydration water from conventional percolation in strict 2D systems can be expected.

Another goal of the present study is to locate the percolation threshold of the hydration water relatively to the coexistence curve of the layering transition (quasi-2D condensation). It is expected, that the line of percolation transitions [13] of so-called physical clusters [14,15] should meet the thermodynamic phase transition at the critical point which is also a percolation point. This line was indeed observed for 2D and 3D Ising lattices [13,16], for the 3D lattice gas [17] and for the Lennard-Jones fluid [18].

In this paper we present the first computer simulation study of the quasi-2D percolation transition of water molecules adsorbed at smooth planar hydrophilic surfaces. To locate the percolation transition, the water clustering

with increasing surface coverage is analyzed above the critical temperature of the layering transition. Peculiarities of the water percolation at hydrophilic spherical surfaces are discussed.

2 Methods

The percolation transition of adsorbed TIP4P water molecules [19] was studied by constant-volume Monte Carlo (MC) simulations, using asymmetric slit-like pores, formed by a smooth hydrophilic wall and by a hard wall. The water-surface interaction with the hydrophilic wall was described by a (9-3) Lennard-Jones potential between the water oxygen and the wall with $\sigma = 2.5 \text{ \AA}$ and a well-depth $U_0 = -4.62 \text{ kcal/mol}$. The chosen potential is strong enough to provide a layering transition of water at this surface. The coexistence curve of this layering transition was obtained previously by MC simulations in the Gibbs ensemble [20].

The clustering of the water molecules was analyzed at several state points with $T = 425 \text{ K}$, i.e. above the critical temperature of the layering transition at this surface ($T_c \approx 400 \text{ K}$ [20]). Simulations were performed in cubic boxes with three different edge lengths: $L = 80, 100$ and 150 \AA . The surface coverage $C = N/L^2$ was varied by putting various numbers N of water molecules in the simulation boxes. Periodic boundary conditions were applied in two directions parallel to the pore walls. Note, that the high localization of the water molecules in the vicinity of the hydrophilic wall was not sensitive to the variation of the width of the pore and edge length L of the box.

Water molecules were considered to belong to the same cluster if they are connected by a continuous path of hydrogen-bonds (H-bond) [1,6,8,21]. An H-bond between two water molecules was assumed to exist, when the distance between the oxygen atoms is $< 3.5 \text{ \AA}$ and the water-water interaction energy is $< -2.4 \text{ kcal/mol}$. Various cluster properties were analyzed after every 1000th MC step and up to 1 million configurations were analyzed for each surface coverage C . Each configuration was inspected to detect the possible presence of an "infinite" cluster, which spans the periodic simulation box at least in one direction parallel to the hydrophilic wall. Then the probability to observe such a spanning cluster R was determined at each surface coverage. The occurrence frequency of water clusters of various sizes S was described by the cluster size distribution n_S . The mean cluster size was calculated as $S_{mean} = \Sigma n_S S^2 / \Sigma n_S S$, where the largest cluster was excluded from the sums. $n_S S / \Sigma n_S S$ is the probability that a given water molecule is member of a finite cluster of size S .

We also analyzed some properties of the largest cluster (of size S_{max}). Firstly

there is the size distribution $P(S_{max})$ of the largest cluster. At the percolation threshold the largest cluster should be a fractal object with a specific fractal dimension. The statistical self-similarity of infinite fractals leads to the following relationship between mass $m(r)$ and linear size r :

$$m(r) \sim r^{d_f} \tag{1}$$

where d_f is the fractal dimension. In our analysis of the fractal dimension of the largest water cluster, $m(r)$ is the number of water molecules which belong to this cluster and which are located inside a sphere of radius r around at a randomly chosen water molecule of the same cluster. We determined the distributions $m(r)$ for each water molecule of the largest cluster of the configuration and averaged them for each surface coverage. The fractal dimension d_f was determined from the fits of the data to equation (1) in the range $r < L$ for each simulated system.

The percolation threshold, when a spanning cluster appears in an infinite system, can be considered to mark the lowest possible concentration, furnishing a full surface coverage. To locate the percolation threshold of water adsorbed on a hydrophilic surface, we used several criteria. Right at the percolation threshold the cluster size distribution n_S obeys the universal power law $n_S \sim S^{-\tau}$, with exponents $\tau = 187/91 \approx 2.05$ [22] and $\tau \approx 2.2$ [23] in the case of random 2D and 3D percolation, respectively. The mean cluster size S_{mean} diverges at the percolation threshold in an infinite system and passes through a maximum when approaching the threshold in a finite system. The fractal dimension of the largest cluster at the percolation threshold is lower than the Euclidean dimension of the system and equal to $d_f^{2D} = 91/48 \approx 1.896$ and $d_f^{3D} \approx 2.53$ in the case of 2D and 3D percolation, respectively [22,23]. Note, that at the critical point of the 2D Ising model, which is a tricritical point for correlated percolation, the fractal dimension of the largest cluster is about 1.95 (187/96) which is higher than $d_f = 187/91$ for random percolation [24]. However, we may neglect a possible trend toward tricriticality in our simulations performed at 25 K above the critical temperature.

3 Results

The coexistence curve of the quasi-2D layering transition of water near the studied hydrophilic surface, obtained by MC simulations in the Gibbs ensemble, is shown in Figure 1 for a slitlike pore of a width $H = 24 \text{ \AA}$. Simulations of layering transitions in various pores with the same water-wall interaction show weak sensitivity of the coexistence curve to the pore shape and width (see Figure 11 in [20] and Figure 72 in Ref.[25]). The shape of the coexistence curve

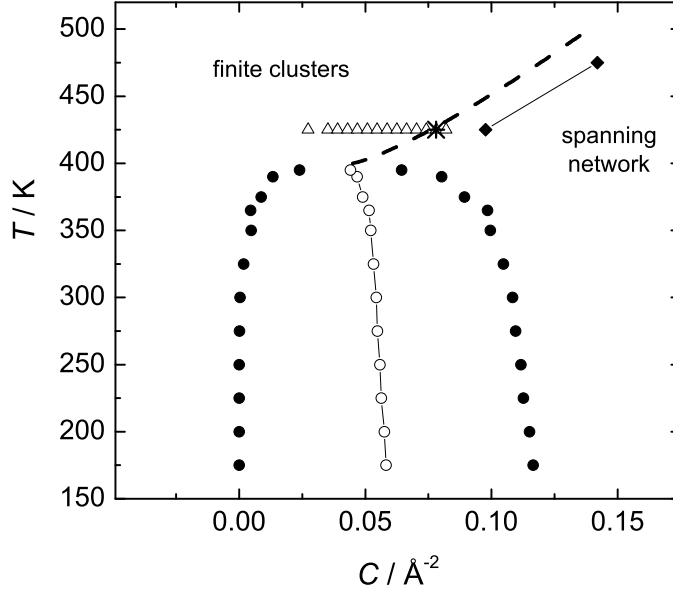


Fig. 1. Coexistence curve (solid circles) and diameter (open circles) of the layering transition of water [20] in terms of number of molecules per unit surface area C . The state points, where water clustering was studied at $T = 425$ K in the system with $L = 80$ Å, are shown by open triangles. The percolation threshold and a possible percolation line are shown by the star and the dashed line, respectively. Percolation thresholds at the surface of a hydrophilic sphere of radius $R_{sp} = 15$ Å are shown by solid diamonds.

of the layering transition of water in a wide temperature range corresponds to the 2D Ising model and the critical temperature is estimated as ≈ 400 K for the used water-wall interaction potential [20,25]. Extrapolation of the coexistence curve diameter (average surface coverage in the two coexisting phases) to the critical temperature gives the critical surface coverage of the layering transition $C_c \approx (0.045 \pm 0.003)$ Å $^{-2}$. To locate a percolation threshold, an analysis of the water clustering was performed at $T = 425$ K in the range of surface coverage C from 0.027 to 0.090 Å $^{-2}$ (see Figure 1). From 175 to 1800 water molecules were placed in the simulation box. The state points, studied in the case of the smallest surface with $L = 80$ Å, are shown by triangles in Figure 1.

The percolation threshold can be located based on the analysis of the cluster size distributions n_S . At low surface coverage most of the water molecules belong to small clusters and n_S shows a rapid exponential decay with increasing S . Upon increasing the hydration level a hump appears in n_S at large S ($C = 0.047$ Å $^{-2}$ in Figure 2). This hump reflects the truncation of the large clusters due to the finite size of the simulated system. At the percolation threshold the cluster size distribution n_S follows the power law behavior $\sim S^{-\tau}$ in the widest range of cluster sizes with $\tau = 2.05$ for 2D percolation. Figure 2 evidences that the percolation threshold of the adsorbed water at the plane with $L = 80$ Å

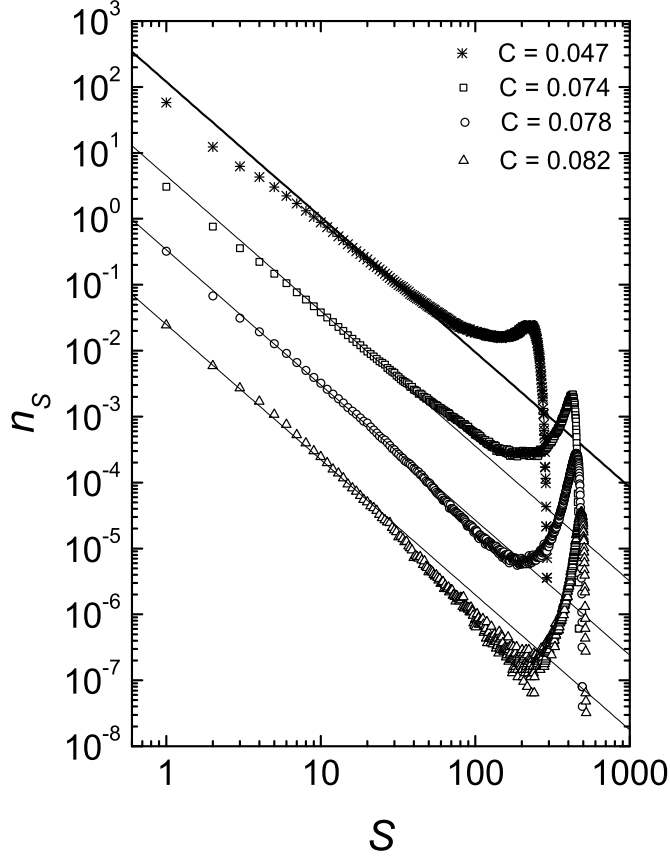


Fig. 2. Probability distribution n_S of clusters with S water molecules for several surface coverages C (in \AA^{-2}) below and above the percolation threshold $C_0 \approx 0.078 \text{\AA}^{-2}$ at the plane with $L = 80 \text{\AA}$). The critical power law $n_S \sim S^{-2.05}$ is shown by the solid lines. The distributions are shifted vertically by one order of magnitude consecutively.

occurs close to the surface coverage $C = 0.078 \text{\AA}^{-2}$ or slightly below. When crossing the percolation threshold, deviations of n_S from the power law at large S before the hump, change the sign from positive to negative (compare $C = 0.074$ and 0.078\AA^{-2} in Figure 2). The negative deviations of n_S increase rapidly with increasing hydration above the percolation threshold ($C = 0.082 \text{\AA}^{-2}$).

A similar behavior of n_S is observed for the two other studied planar surfaces with $L = 100$ and 150\AA . The percolation threshold is estimated at a coverage C close to 0.070\AA^{-2} for the plane with $L = 100 \text{\AA}$ and close to 0.078 for the plane with $L = 150 \text{\AA}$. The distributions n_S close to the percolation threshold are compared for three studied planar surfaces in Figure 3. Note, that the variation of the surface coverage for the plane with $L = 100 \text{\AA}$ by 0.01\AA^{-2} near the coverage $C = 0.070 \text{\AA}^{-2}$ was rather coarse. Therefore, we conclude that the threshold surface coverage C_0 obtained from the distributions n_S , is

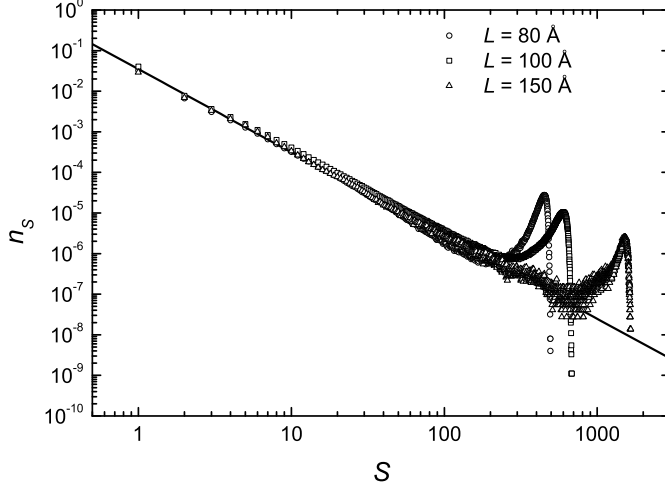


Fig. 3. Probability distribution n_S of clusters with S water molecules at planar surfaces of various sizes at surface coverages close to the percolation thresholds: $C = 0.078 \text{ \AA}^{-2}$ (circles), 0.070 \AA^{-2} (squares) and 0.078 \AA^{-2} (triangles). The critical power law $n_S \sim S^{-2.05}$ is shown by a solid line.

almost indistinguishable for the three studied surfaces and can be estimated as $\approx 0.078 \text{ \AA}^{-2}$.

Various properties of water clusters at the planar surface with $L = 80 \text{ \AA}$ are shown in Figure 4. The mean cluster size S_{mean} shows a shallow maximum at a surface coverage of about $C \approx 0.065 \text{ \AA}^{-2}$, i.e. below the percolation threshold C_0 . The same behavior of S_{mean} is observed also for the other studied planar surfaces, in agreement with percolation theory. The fractal dimension of the largest cluster d_f is close to the value of the 2D percolation $d_f^{2D} = 91/48 \approx 1.896$ at the threshold surface coverage C_0 (see Figure 4, lower panel). This fact indicates the 2D character of the percolation transition of the adsorbed water. Values of d_f at various hydration levels for the three studied surfaces are compared in Figure 5 (lower panel). Evidently, d_f achieves the threshold value d_f^{2D} at about the same surface coverage C_0 , independent from the size of the studied surface. This allows two conclusions: i) adsorbed water shows a 2D percolation threshold at $C_0 \approx 0.078 \text{ \AA}^{-2}$ and ii) the cluster size distribution n_S and the fractal dimension of the largest cluster d_f at the percolation threshold are not very sensitive to the size of the simulated system.

The percolation threshold can also be located based on the spanning or wrapping probability R , which is the probability to observe a spanning (percolating) cluster in a finite system of size L . This probability can be defined in various ways, which are called spanning rules. For instance, for 2D lattices there is R^1 , the probability, that a cluster spans in one direction *only* (horizontally or vertically), R^e , the probability that the clusters spans *either* horizontally or vertically (or both), etc. In the present paper we used the spanning rule R^e to define a spanning probability. The dependency of the spanning probability

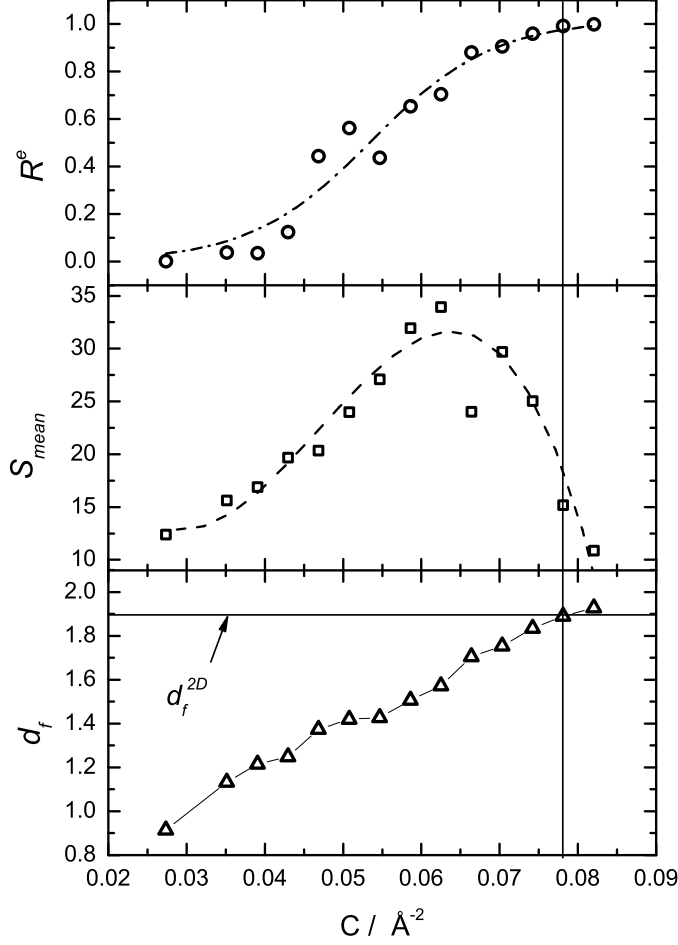


Fig. 4. 2D percolation transition of water at the planar surface with $L = 80 \text{ \AA}$. Spanning probability R (circles, upper panel), mean cluster size S_{mean} (squares, middle panel) and fractal dimension of the largest cluster d_f (triangles, lower panel) are shown as function of water surface coverage C . The dot-dashed line is a fit of R by the Boltzmann function. The dashed line is a guide for eyes only. The vertical line indicates the threshold water coverages C_0 estimated from the behavior of n_S .

on the occupancy variable (surface coverage) is shown in Figures 4 and 5 for different system sizes. The variation of R is steeper in larger systems.

The dependency of the spanning probability R on the occupancy C for various system sizes should cross at the percolation threshold. The value of R at this crossing point depends on the spanning rule and on the dimensionality of the system, but should not depend on lattice structure, type of percolation (site or bond percolation), etc. [26]. Figure 5 evidences that the $R^e(C)$ for water adsorbed at surfaces of various size do not cross exactly in one point. The application of a sigmoidal (Boltzmann function) fit allows to locate the crossing point for the two smallest surfaces at about $R^e \approx 0.7$. However, $R^e(C)$ for the largest surface ($L = 150 \text{ \AA}$) seems to be rather separated and meets $R^e(C)$ for the smallest surface only when $R^e > 0.9$. Note, that the value of

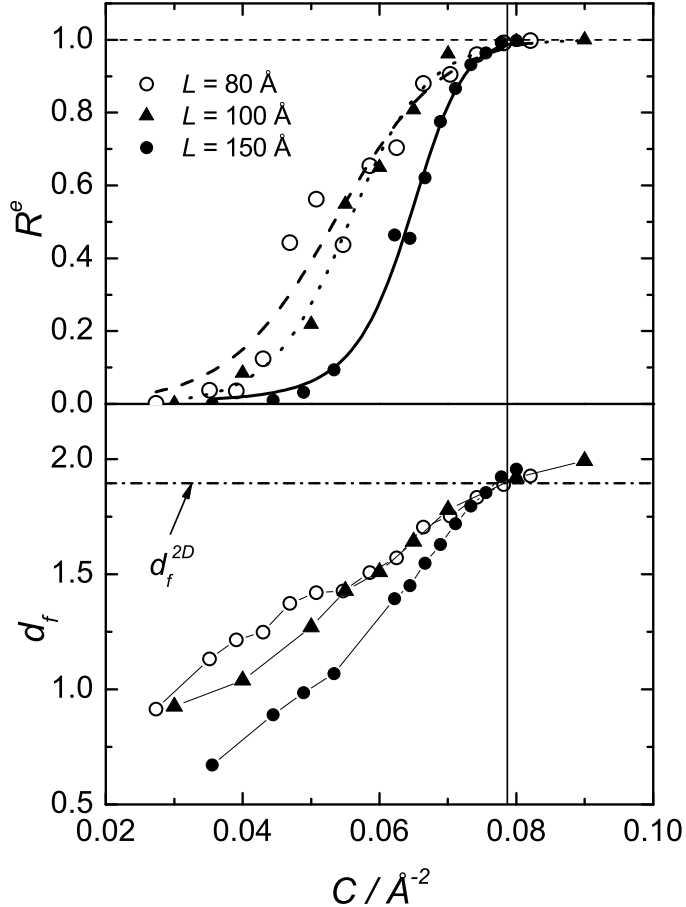


Fig. 5. Spanning probability R (upper panel) and fractal dimension of the largest water cluster d_f (lower panel) as functions of the surface coverage C at the planar hydrophilic surfaces of various sizes. The fits of R by the Boltzmann function are shown for the smallest, middle and largest planar surfaces by dashed, dotted and solid lines, respectively. The threshold surface coverage $C_0 \approx 0.078 \text{ \AA}^{-2}$ is shown by a vertical line.

the spanning probability at the threshold coverage $C_0 \approx 0.078 \text{ \AA}^{-2}$, obtained above from the behavior of n_S and d_f , exceeds 0.95 for all studied surfaces.

The probability distributions $P(S_{max})$ of the size S_{max} of the largest water cluster at the surface with $L = 80 \text{ \AA}$ are shown in Figure 6 for several surface coverages C . At low hydration levels, $P(S_{max})$ has only a single maximum at low S_{max} (Figure 6, upper panel). With increasing surface coverage $P(S_{max})$ shows a characteristic two-peak structure (middle panels) which remains noticeable close to the percolation threshold (lower panel). We have found, that the left peak is due to non-spanning largest clusters, whereas the right peak is due to spanning largest clusters. The two contributions to $P(S_{max})$ are shown in Figure 7 for the planar surface with $L = 100 \text{ \AA}$ at the surface coverage where R is about 50 %.

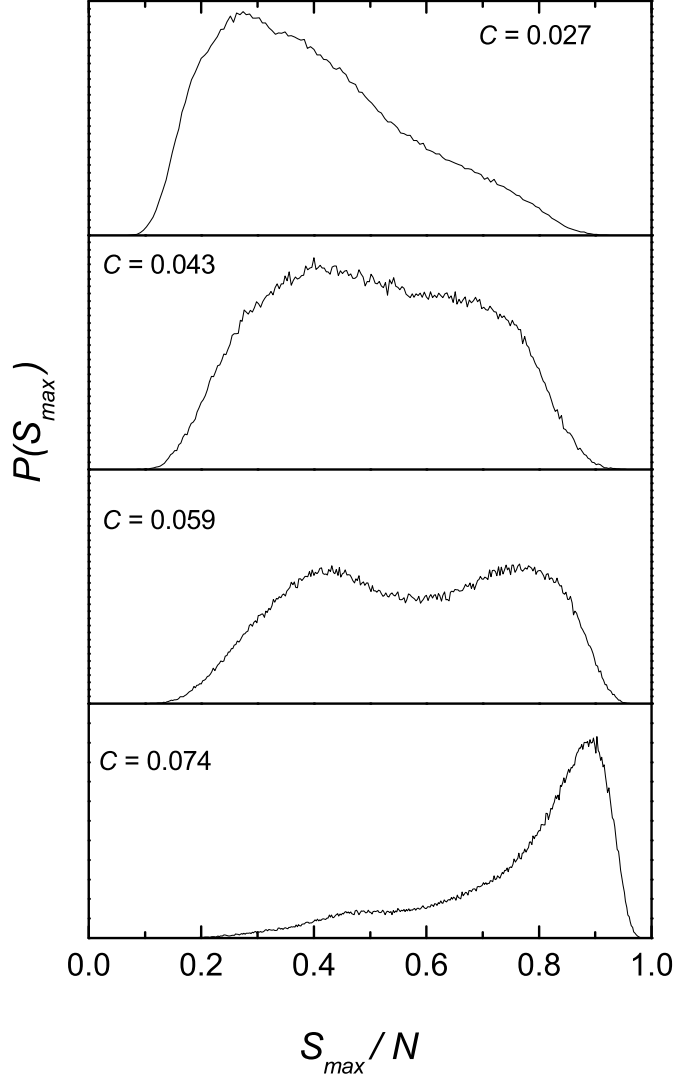


Fig. 6. Probability distribution $P(S_{max})$ of the size S_{max} of the largest water cluster at the planar surface with $L = 80 \text{ \AA}$ at various surface coverages C (in \AA^{-2}) normalized on the total number of water molecules N .

We have calculated the average sizes of spanning S_{span}^{av} and nonspanning S_{non}^{av} largest clusters at various hydration levels. Their ratio shows no clear dependence on the system size and a weak tendency to increase with increasing surface coverage (see Figure 8). The ratio $S_{span}^{av}/S_{non}^{av}$ can be well defined at the hydration level, where spanning and non-spanning largest clusters have comparable probabilities. In this range $S_{span}^{av}/S_{non}^{av}$ is about 1.8 for all studied planes.

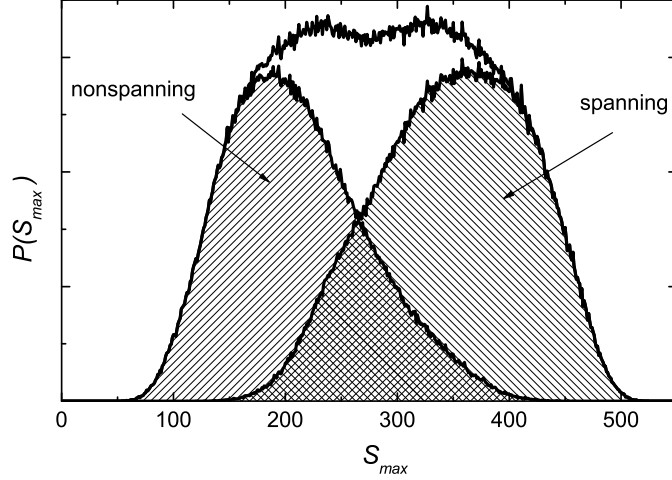


Fig. 7. Probability distribution $P(S_{max})$ of the size S_{max} of the largest water cluster clusters at the planar surface with with $L = 100 \text{ \AA}$ at the surface coverages $C = 0.055 \text{ \AA}^{-2}$, where spanning and nonspanning largest clusters exists with comparable probabilities. Size distributions of spanning and nonspanning largest clusters normalized on their respective probabilities, are shown as two dashed areas.

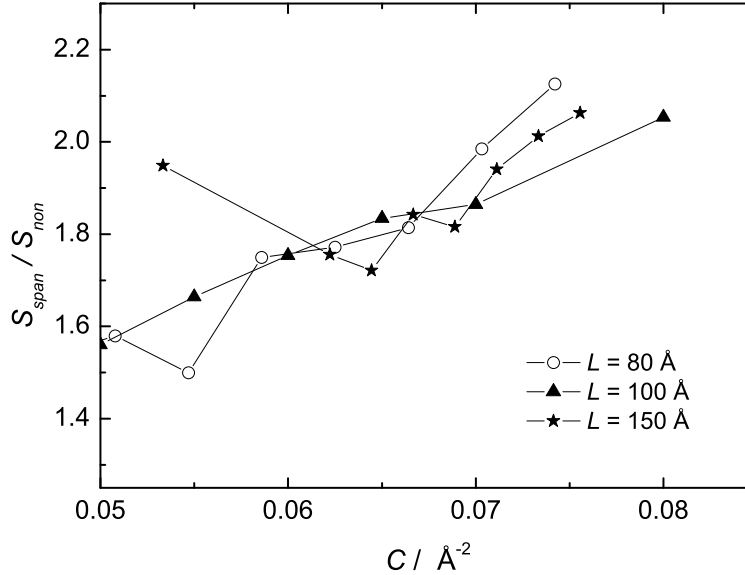


Fig. 8. Ratio of the average sizes of spanning S_{span}^{av} and nonspanning S_{non}^{av} largest water clusters as a function of surface coverage.

4 Discussion

Water adsorbed at smooth hydrophilic surfaces shows a well defined percolation transition at temperatures above the critical temperature of the layering transition. The fractal dimension of the largest cluster d_f at the percolation threshold, which is located by the power-law behavior of the cluster size distribution n_S , evidences the 2D character of the percolation transition. The

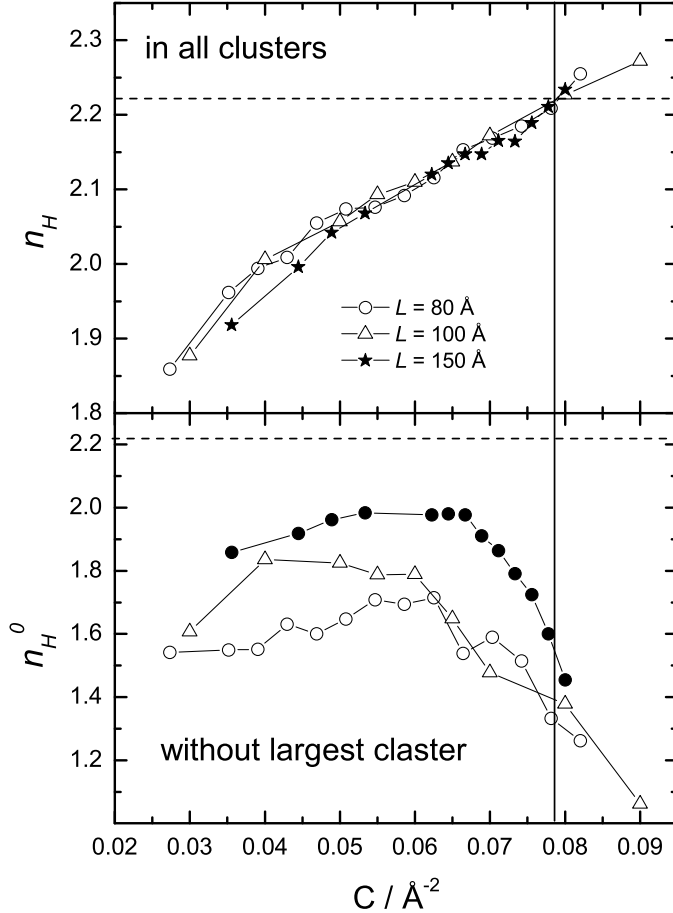


Fig. 9. Average number of hydrogen bonds, formed by each water molecule, as a function of surface coverage, calculated for all water molecules (n_H : upper panel) and for molecules, which do not belong to the largest cluster (n_H^0 : lower panel).

surface coverage at the percolation threshold does not change noticeably with system size and we estimate it as $C_0 \approx 0.078 \text{ \AA}^{-2}$ at $T = 425 \text{ K}$. The spanning probabilities R^e for various system sizes intersect in one point at a surface coverage C , which is close to the percolation threshold value.

Nevertheless, the behavior of the spanning probability R for the adsorbed water differs from that observed in conventional percolation studies of 2D lattices and continuous systems. For the definition of the spanning probability R^e used in the present paper, values R^e at the intersection point were obtained from 0.69 [27,28] to 0.81 [26] for 2D lattices and from 0.64 for percolation of hard and soft discs [29] to ~ 0.7 for 2D polymers [30]. The spanning probability at the intersection point in the case of adsorbed water ($R^e > 0.95$) is noticeably higher than in strictly 2D systems. Note, that the opposite trend should be expected due to the quasi-2D character of the simulated system: R at the percolation threshold on 3D lattices is ~ 0.5 [27], i.e. lower than in 2D systems.

The obtained threshold water coverage is roughly about 70% of a water liq-

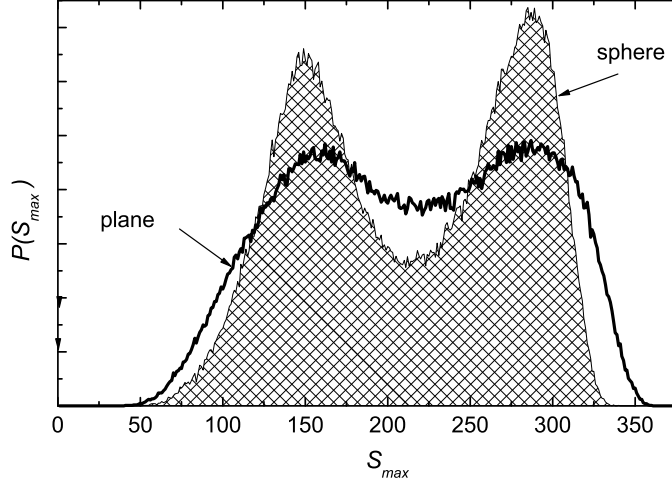


Fig. 10. Probability distribution $P(S_{max})$ of the size S_{max} of the largest water cluster at the planar surface with $L = 80 \text{ \AA}$ and $N = 350$, compared with $P(S_{max})$ at the surface of a hydrophilic sphere of radius $R_{sp} = 15 \text{ \AA}$ and $N = 375$ (dashed area).

uid monolayer, which is characterized by a surface coverage $C \approx 0.11 \text{ \AA}^{-2}$ at ambient temperature (see Figure 1). Taking into account, that for the studied systems the fraction of water molecules which stick out of the first surface layer does not exceed 5% [31], we may conclude, that at the percolation threshold water covers about $2/3$ of the surface. It covers the whole surface more or less "homogeneously" but by a ramified fractal, which needs only $2/3$ of the material of monolayer. This threshold surface coverage can be compared with the threshold value of the occupancy variable in 2D lattice models. The honeycomb lattice with 3 neighbors and the square lattice with 4 neighbors seem to be the most relevant to water adsorbed at a hydrophilic surface [25,32]. For these lattices the threshold values of the occupancy variable are ≈ 0.70 and ≈ 0.59 for site percolation and ≈ 0.65 and 0.5 for bond percolation, respectively [22]. So, quasi-2D correlated site-bond percolation of adsorbed water occurs at a threshold occupancy, which is rather close to the thresholds for random site and bond percolation in 2D lattices. On the other hand, water coverage at the threshold is smaller than the corresponding value (≈ 0.85 [29]) for the random percolation of hard (non-overlapping) discs at the surface. Note, that the occupancy variables discussed above refer to closed packing of discs and should not be mixed with so-called space occupation probability, which is ≈ 0.45 at the threshold for 2D site percolation in various lattices [33] (see paper [11] for more details). So, we have found a strong similarity of the percolation transition of the adsorbed quasi-2D water with conventional percolation in 2D lattices. Note, that site-bond percolation transition in bulk liquid water was found to be similar to the percolation transition in 3D diamond lattice [1,2].

To examine the possible location of the line of water percolation transitions relatively to the coexistence region of the layering transition we used our studies of the percolation threshold at the surface of a sphere [11,31]. The

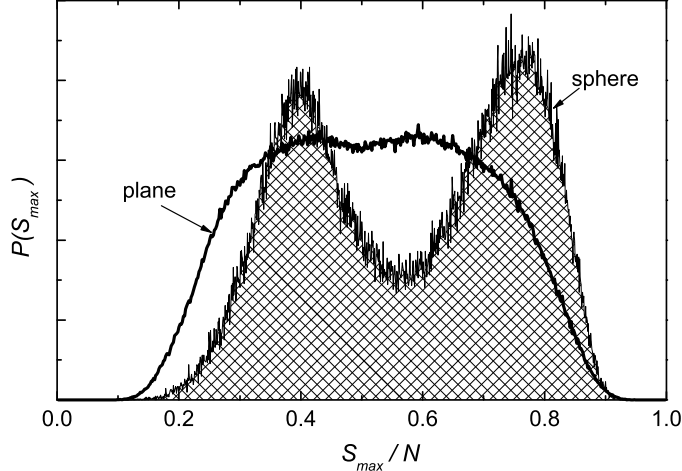


Fig. 11. Probability distribution $P(S_{max})$ of the size S_{max} of the largest water cluster at the planar surface with $L = 100 \text{ \AA}$ (line, shown also in Figure 7) is compared with $P(S_{max})$ at the surface of a hydrophilic sphere of radius $R_{sp} = 30 \text{ \AA}$ at $C = 0.088 \text{ \AA}^{-2}$ (dashed area).

location of the water percolation threshold at $T = 425$ and 475 K at the surface of a sphere with radius $R_{sp} = 15 \text{ \AA}$ is shown in Figure 1 (solid diamonds). The shift of the percolation threshold at the spherical surface toward higher values of surface coverage is due to an increasing number of water molecules in the second hydration shell (see Ref. [31]). The opposite trend is expected for the percolation transition on the inner surface of a cylinder, where indeed the layering transition is found slightly shifted towards lower surface coverages [25]. Taking into account, that the shift of the percolation threshold of surface water with temperature is rather universal for various surfaces [31], we may schematically draw the line of the percolation transitions of water at the planar surface, as it is shown in Figure 1. Obviously, our results are consistent with the theoretical expectations [13,14] and with the results of simulations of the lattice gas and LJ fluids, which show that the line of percolation transitions meets the coexistence curve at the critical point [17,18].

At subcritical temperatures, the percolation transition can be prevented by phase separation, which appears as the formation of droplets of the second phase. In computer simulations, however, the formation of droplets is hampered by the finite size of the simulated systems and the second phase can be detected only deeply inside the two-phase region [34].

The relative insensitivity of the percolation threshold of hydration water to the size of the studied system is very helpful, since it allows meaningful studies of percolation in rather small systems. Simulations with just a few hundred water molecules are enough to accurately locate a 2D percolation threshold. This fact, which is especially useful for the study of networks of the surface water in biological systems, obviously originates from the invariance of water

clustering and percolation in terms of the number of water-water hydrogen bonds [31].

Figure 9 shows the average number of water-water H-bonds in the three studied systems at various hydration levels, when averaging was performed over all clusters (n_H , upper panel) and when the largest cluster was excluded from consideration (n_H^0 , lower panel). Evidently, the finite-size effect is noticeable for non-largest clusters only. The percolation threshold for all planes is located at $n_H = 2.22$ and this value varies no more on ± 0.1 for other temperatures and systems, including biosystems [31].

Finally, we would like to discuss the two-peak structure of the size distribution of the largest cluster $P(S_{max})$ shown in Figures 6 and 7. This structure was observed recently for 2D lattice models [35]. The ratio $S_{span}^{av}/S_{non}^{av}$ for lattices was found between 1.6 and 1.7 with some week dependence on dimensionality. We observed a slightly higher value of this ratio of about 1.8, which indicates a larger difference between the sizes of the spanning and nonspanning largest clusters in the continuous system. With increasing system size the two-peak structure of $P(S_{max})$ becomes less and less pronounced. As the ratio $S_{span}^{av}/S_{non}^{av}$ does not depend on the size of simulated plane (see Figure 8), this effect should be attributed to the increase of the width of the distributions of spanning and non-spanning largest clusters.

The two-peak structure of $P(S_{max})$ is strongly enhanced at spherical surfaces [11,12]. In Figure 10, we compare $P(S_{max})$ for the plane with $L = 80 \text{ \AA}$ and for the spherical surface of radius $R_{sp} = 15 \text{ \AA}$ with approximately the same number of adsorbed water molecules ($N = 350$ and 375 , respectively). Evidently, the distributions of the spanning and nonspanning largest clusters are much narrower at the spherical surface. Besides, the ratio $S_{span}^{av}/S_{non}^{av}$ is about 2 in the latter case. Both factors can be responsible for the enhancement of the two-peak structure of $P(S_{max})$ at the spherical surface.

One peculiarity of the spherical surface reported in reference [12] is the independence (or weak dependence) of the two-peak structure of $P(S_{max})$ on the surface size. In Figure 11 we compare $P(S_{max})$ for the planar and for the spherical surface with comparable surface area $\sim 10000 \text{ \AA}^2$ at the surface coverages, where the spanning and non-spanning configurations have roughly equal probabilities. Comparison of Figures 10 and 11 shows, that the two-peak structure of $P(S_{max})$ diminishes with increasing size of the plane, whereas this is not the case for spheres. The ratio $S_{span}^{av}/S_{non}^{av}$ was also found insensitive to the size of the sphere and remains about 2 for spheres of radius 15, 30 and 50 \AA [11]. This phenomenon indeed deserves further studies. The enhancement of the two-peak structure at spherical surfaces has an important consequence: the spanning and non-spanning clusters can be distinguished even in cases, where a spanning cluster can not be defined in the conventional way. The

pronounced two-peak structure of $P(S_{max})$ allows the separation of spanning and non-spanning clusters at the surface of other finite objects, for example, at the surface of biomolecules [11,12].

References

- [1] Geiger A, Stillinger F H and Rahman A 1979 *J. Chem. Phys.* **70** 4185
- [2] Blumberg R L, Stanley H E, Geiger A and Mausbach P 1984 *J. Chem. Phys.* **80** 5230
- [3] Guissani Y and Guillot B 1993 *J. Chem. Phys.* **98** 8221
- [4] Kalinichev A G and Bass J D 1997 *J. Phys. Chem A* **101** 9720
- [5] Partay L and Jedlovszky P 2005 *J. Chem. Phys.* **123**
- [6] Oleinikova A, Brovchenko I, Geiger A and Guillot B 2002 *J. Chem. Phys.* **117** 3296
- [7] Dougan L, Bates S P , Hargreaves R, Fox J P, Crain J, Finney J L, Reat V and Soper A K 2004 *J. Chem. Phys.* **121** 6456
- [8] Brovchenko I, Geiger A and Oleinikova A 2004 *Phys. Chem. Chem. Phys.* **6** 1982
- [9] Rupley J A and Careri G 1991 *Adv. Protein Chem.* **41** 37
- [10] Haranczyk H 2003 *On water in extremely dry biological systems* Wydawn. Univ. Jagiellonskiego, Krakow, Poland
- [11] Oleinikova A, Smolin N, Brovchenko I, Geiger A and Winter R 2005 *J. Phys. Chem. B* **109** 1988
- [12] Smolin N, Oleinikova A, Brovchenko I, Geiger A and Winter R 2005 *J. Phys. Chem. B* **109** 10995
- [13] Kertesz J 1989 *Physica A* **161** 58
- [14] Coniglio A and Klein W 1980 *J. Phys. A: Math. Gen.* **13** 2775
- [15] Pugnaloni L A and Vericat F 2002 *J. Chem. Phys.* **116** 1097
- [16] Coniglio A, Nappi C R, Peruggi F and Russo L 1977 *J. Phys. A: Math. Gen.* **10** 205
- [17] Campi X, Krivine H and Krivine J 2003 *Physica A* **320** 41
- [18] Campi X, Krivine H and Sator N 2001 *Nucl. Phys. A* **681** 458c
- [19] Jorgensen W L, Chendrasekhar J, Mwdura J D, Impey R W and Klein M L 1982 *J. Chem. Phys.* **77** 926

- [20] Brovchenko I, Geiger A and Oleinikova A 2004 *J. Chem. Phys.* **120** 1958
- [21] Geiger A and Stanley H E 1982 *Phys. Rev. Lett.* **49** 1895
- [22] Stauffer D 1985 *Introduction to Percolation Theory*; Taylor and Francis: London and Philadelphia.
- [23] Jan N 1999 *Physica A* **266** 72
- [24] Stella A L and Vanderzande C 1989 *Phys. Rev. Lett.* **62** 1067
- [25] Brovchenko I and Oleinikova A 2005 In *Handbook of Theoretical and Computational Nanotechnology*; American Scientific Publishers.
- [26] Hovi J P and Aharony A 1996 *Phys. Rev. E* **53** 235
- [27] Martins P H L and Plascak J A 2003 *Phys. Rev. E* **67** 046119
- [28] Newman M E J and Ziff R M 2001 *Phys. Rev. E* **64** 016706
- [29] Hu C K 1999 *Proc. Natl. Sci. Counc. ROC(A)* **23** 331
- [30] Munkel C and Heermann D W 1993 *Physica A* **199** 12
- [31] Oleinikova A, Brovchenko I, Smolin N, Krukau A, Geiger A and Winter R 2005 cond-mat/0505564
- [32] Brovchenko I and Geiger A 2002 *J. Mol. Liq.* **96-97** 195
- [33] Zallen R and Scher H 1971 *Phys. Rev. B* **4** 4471
- [34] MacDowell L G, Virnau P, Muller M and Binder K 2004 *J. Chem. Phys.* **120** 5293
- [35] Sen P 2001 *J. Phys. A: Math. Gen* **34** 8477